Downloaded by UNIV OF GUELPH LIBRARY on October 1, 2011 | http://pubs.acs.org
Publication Date (Web): September 2, 2011 | doi: 10.1021/bk-2011-1071.ch004

## Chapter 4

# Thermodynamic Control on Terminal Electron Transfer and Methanogenesis

**Christian Blodau***

**School of Environmental Sciences, University of Guelph, N1G 2W1, Guelph, Canada**
***christian.blodau@uni-muenster.de; present address: Hydrology Group, ILÖK, University of Münster, Germany**

Terminal electron accepting processes (TEAPs) control the fate of elements in anoxic environments. This study focuses on thermodynamic regulation of $H_2$-dependent TEAPs. $H_2$-dependent methanogenesis and sulfate reduction operate near free energy thresholds ($\Delta G_c$) and can be inhibited by changes in thermodynamic conditions, whereas more 'potent' TEAPs occur far from their energy thresholds and lower $H_2$ concentrations to levels that exclude other TEAPs. Metabolic free energy thresholds depend on microbial physiology and occur when the energy conserved by ATP generation approaches the thermodynamic driving force. A model analysis for peat-sand mixtures suggests that acetoclastic methanogenesis can be inhibited by $CH_4$ and dissolved inorganic carbon (DIC) accumulation, lowering the free energy ($\Delta G_r$) toward an energy threshold ($\Delta G_c$), which was identified by inverse modeling near - 25 kJ $mol^{-1}$. Inhibition was sensitive to $\Delta G_c$ and acetate concentrations, so that $\Delta G_c \pm 5$ kJ $mol^{-1}$ and a range of 1 to 100 µmol $L^{-1}$ acetate lead to strongly differing steady state $CH_4$ concentrations in the model results.

## Introduction and Review

### Terminal Electron Transfer and the Role of Molecular Hydrogen

The distribution of chemical species in anoxic environments is governed by microbially mediated electron transfer, and in particular by terminal electron

© 2011 American Chemical Society
In Aquatic Redox Chemistry; Tratnyek, P., et al.;
ACS Symposium Series; American Chemical Society: Washington, DC, 2011.

accepting processes and methanogenesis (*1*, *2*) (Table 1). Geochemists have recognized early that thermodynamic considerations may provide a framework for analyzing the occurrence of TEAPs in sediments (*3*). From such origins and the investigation of the bioenergetic regulation and limits of anerobic metabolism (*4–6*), the role of molecular hydrogen as regulator for TEAPs, methanogenesis, and syntrophic fermentation processes was elucidated. More recently, coherent and quantitative concepts addressing the regulation of TEAPs in anoxic environments have been developed (*7*). Efforts are also undertaken to integrate such concepts into reactive transport and diagenetic models (*8*). This study's objective is to summarize some of this progress and to analyze how constraints on energy and solute transport may control the kinetics of microbially mediated electron transfer processes in anoxic environments. The latter objective is also addressed based on a simple methanogenic, diffusion dominated system.

Downloaded by UNIV OF GUELPH LIBRARY on October 1, 2011 | http://pubs.acs.org
Publication Date (Web): September 2, 2011 | doi: 10.1021/bk-2011-1071.ch004

Anaerobic decomposition of both immobile and dissolved organic matter proceeds through the action of extracellular enzymes, fermentation, syntrophic processes, and TEAPs (*9*) (Fig. 1). Decomposition is initially controlled by the activity of extracellular enzymes, which are produced by fermenting bacteria, and hydrolyzed polymers that cannot pass the outer membrane of microorganisms (*10*). Among many decomposition products, acetate and molecular hydrogen ($H_2$) are primary substrates for methanogenic *Archaea* and a range of microorganisms mediating TEAPs (*11*). For simplicity, methanogenesis is included under the TEAP heading. Molecular $H_2$ plays a particularly important role in the anaerobic decomposition network. The microbial demand for $H_2$ is strong since the ability to oxidize $H_2$ through membrane-bound hydrogenases is phylogenetically widespread (*12*), linking $H_2$ to reduction of widespread electron acceptors such as $NO_3^-$, $SO_4^{2-}$, and $CO_2$, and to less common acceptors, such as As(V) and U(VI) (see also (*13*) and (*14*)). Thus, its concentration controls much of the energy available to TEA bacteria. $H_2$ typically has a half-life of less than a minute (*15*), which allows for rapid concentration adjustment with changing environmental conditions (*11*). The free energy of oxidation of $H_2$ is also highly dependent on $H_2$ activity because it involves only a transfer of two electrons. This network of processes involving $H_2$ transfer is subjected to constraints by transport of solutes and gases, microbial kinetics, stoichiometric limitations, and the availability of Gibbs free energy in form of electron donors and acceptors (Figure 1). The level of energy available results from fluxes of oxidants and reductants, and the rate at which mobile reactants are supplied, as analyzed by Kurtz and Peiffer (*16*) in this volume.

Lovley and Goodwin (*17*) recognized the role of $H_2$ in anaerobic decomposition networks and suggested its use as a redox indicator in studying competition between TEAPs. The authors originally argued that $H_2$ concentration under steady-state conditions should depend only on physiological characteristics of hydrogenotrophic microorganisms, i.e. the growth yield (Y) and the half-saturation constant (K) for $H_2$ uptake, which tend to increase and decrease, respectively, with increasing energy yield of a given TEAP. External factors, such as the $H_2$ supply rate, should not influence $H_2$ concentrations in steady-state systems (*18*). Levels of $H_2$ in anoxic environments, thus, decrease with increasing standard Gibbs free energy of the predominant TEAP. This way, energetically less

potent TEAPs are excluded from substrate utilization as their energy thresholds are exceeded and their metabolism ceases. According to this concept, $H_2$ levels can be used as a redox indicator because levels adjust to ranges that are optimal and indicative for a particular predominating TEAP (*17*, *19*). For a compilation of these ranges the reader is referred to Heimann, et al. (*20*). The approach has been widely used to investigate the microbiology and redox chemistry of pristine and contaminated sediments (*21–24*). Similar observations were made for other low-molecular-weight intermediates (*25*) but concentration levels have been less clear than for $H_2$.

Downloaded by UNIV OF GUELPH LIBRARY on October 1, 2011 | http://pubs.acs.org
Publication Date (Web): September 2, 2011 | doi: 10.1021/bk-2011-1071.ch004

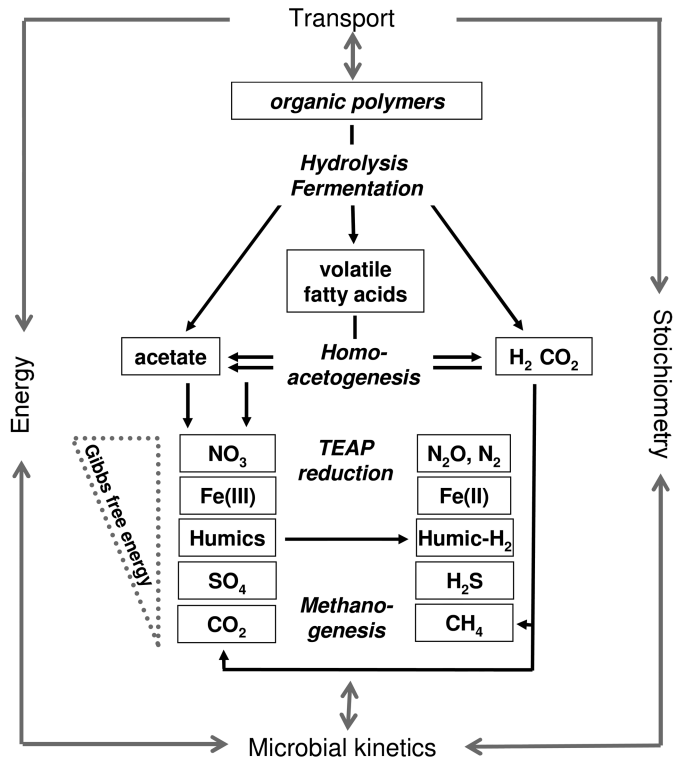



*Figure 1. Simplified network of processes involved in anaerobic organic matter decomposition in anoxic aqueous systems and potential controls by transport, energy, microbial kinetics, and microorganism stoichiometry.*

**Table 1. Overview of important $H_2$-consuming TEAPs and their Gibbs free energies under standard ($\Delta G^0$) and exemplary environmental ($\Delta G_r$) conditions, respectively**

| *Process* | *Reaction stoichiometry* | *$\Delta G^0$ (kJ mol$^{-1}$)*[a] | *$\Delta G_r$ (kJ mol$^{-1}$)*[b] |
|---|---|---|---|
| Oxic respiration | $1/2\ O_2 + H_2 \rightarrow H_2O$ | -237.2 | -206.7 |
| Denitrification | $2/5\ NO_3^- + H_2 + 2/5\ H^+ \rightarrow 1/5\ N_2 + 6/5\ H_2O$ | -240.1 | -186.6 |
| Iron reduction | $2\ FeOOH(a) + H_2 + 4\ H^+ \rightarrow 2\ Fe^{2+} + 4\ H_2O$ | -182.5 | -39.8 |
| Arsenate reduction | $HAsO_4^{2-} + H_2 + 2\ H^+ \rightarrow H_3AsO_3 + H_2O$ | -162.4 | -53.9 |
| Sulfate reduction | $1/4\ SO_4^{2-} + H_2 + 1/4\ H^+ \rightarrow 1/4\ HS^- + H_2O$ | -48.0 | -9.5 |
| Hydrogenotrophic methanogenesis | $1/4\ HCO_3^- + H_2 + 1/4\ H^+ \rightarrow 1/4\ CH_4 + 3/4\ H_2O$ | -43.9 | -8.2 |
| Homoacetogenesis | $1/2\ HCO_3^- + H_2 + 1/4\ H^+ \rightarrow 1/4\ Acetate^- + H_2O$ | -36.1 | +2.4 |

[a] Calculated from Gibbs free energies of formation (*26*–*28*); $O_2$, $H_2$, $N_2$, and $CH_4$ as gaseous species. [b] At the following conditions: T = 25 ºC, $[O_2] = 0.21$, $[N_2] = 0.78$, $[CH_4] = [NO_3^-] = [Fe^{2+}] = [HAsO_4^{2-}] = [H_3AsO^3] = [SO_4^{2-}] = [HS^-] = [Acetate^-] = 10^{-4}$, $[HCO_3^-] = 10^{-2}$, $[H^+] = 10^{-7}$, $[H_2] = 10^{-5}$ (corresponding to an aqueous concentration of approximately 8 nmol L$^{-1}$). Square brackets indicate activities of aqueous species or fugacities of gaseous species. Data have previously been reported in (*29*) and (*20*).

## The Energy Threshold – *in Situ* Energy Concept in Terminal Electron Transfer

Lovley and Goodwin's (*17*) $H_2$-based redox indicator concept did not always predict the occurrence of TEAPs well (*30*–*34*). Often TEAPs were also found to occur simultaneously (*35*, *36*). $H_2$ concentrations in real-world systems are not solely related to the physiology of the $H_2$-consuming microbes but are also influenced by the presence of other electron donors, the concentration levels of electron acceptors, transient environmental conditions, and micro-scale heterogeneity. Redox conditions and electron flow in anoxic systems have, thus, also been analyzed focussing on the *in situ* energy yields of individual processes (*30*, *37*, *38*). Energy yields can be calculated from the activities of substrates and products involved in a process at a given temperature and compared to a theoretical or empirical minimum energy requirement for the process, so called 'energy threshold'. This kind of analysis provides insight into the functioning of an individual electron transfer process. If *in situ* energies are smaller (more positive) than the energy threshold for a particular process, it cannot occur; if energies are much larger than usually observed while the process is ongoing, it is likely inhibited by some other constraint; and if the *in situ* energy of the process approaches its energy threshold it should become increasingly slow.


In Aquatic Redox Chemistry; Tratnyek, P., et al.;
ACS Symposium Series; American Chemical Society: Washington, DC, 2011.

Downloaded by UNIV OF GUELPH LIBRARY on October 1, 2011 | http://pubs.acs.org
Publication Date (Web): September 2, 2011 | doi: 10.1021/bk-2011-1071.ch004

The expectation is that TEAPs operate at *in situ* energy levels that are close to but not at their specific energy thresholds. In agreement with this idea, $\Delta G_r$ for hydrogenotrophic methanogenesis was about -35 kJ $mol^{-1}$ in several anaerobic freshwater systems during ongoing methanogenesis (*39*, *40*), whereas the theoretical energy threshold for the process is believed to be -20 to -25 kJ $mol^{-1}$ under active growth (*5*).

## Energy Thresholds

Energy thresholds have been derived from the ATP synthesis energy. The *in vivo* energy required for synthesis of one mol of ATP is around +50 kJ, depending on intracellular levels of ATP, ADP, phosphate, $Mg^{2+}$, and $H^+$ (*5*, *28*). Additional required thermodynamic driving force can be accounted for by simply adding an energy quantum for the process (*5*) and more generally by including a thermodynamic efficiency factor (*6*, *41*). Since the $H^+$/ATP ratio of the ATP synthase is typically in the range of 3-4 (*42*) the energy threshold equals the energy released by one proton returning into the cell through the ATP synthase. Based on this argument, the energy threshold should be around 1/3 or 1/4 of -70 kJ $mol^{-1}$, i.e. about -20 kJ $mol^{-1}$ of substrate for methanogenesis (*5*). Under starvation conditions, smaller values of -10 to -15 kJ $mol^{-1}$ of substrate may be found (*6*, *41*).

The $H^+$/ATP based energy threshold concept requires some flexibility with regard to methanogenic *Archaea*, which are particularly well-adapted to low energy levels (*43*). *Archaea* actively pump sodium ions across their membranes as a bioenergetic pathway, which may account for part of the ATP that is synthesized (*44*, *45*), and they are characterized by more variable and larger $H^+$/ATP ratios (*43*). Fermentation processes are not subject to the $H^+$/ATP energy threshold concept since ATP is synthesized via substrate level phosphorylation (*46*, *47*). Minimum energy requirements for these processes and acetogenesis were generally found to be smaller than in TEAPs (*46*, *47*). Compilations of minimum free energy yields for various TEAPs and fermentation processes were compiled by Hoehler (*6*) and Kleerebezem and Stams (*48*).

## Differences in Energetic Control on TEAPs

The different levels of Gibbs free energies provided from TEAPs and methanogenesis (Table 1) have been found to correlate with the 'tightness' of thermodynamic control and the *in situ* energies that adjust during an ongoing process. This finding is reflected in the levels of energy thresholds that have been reported, and in the difference between these thresholds and *in situ* energies that were typically attained in anoxic environments. When Gibbs free energy is large, in particular with respect to denitrification, energy thresholds were found to be larger as well (*20*, *37*). Energy conservation per hydrogen consumed has been suggested to be twice or more that of sulfate reduction and methanogenesis, based on the energy conservation mechanisms; energy thresholds should accordingly be proportionately higher and attained when hydrogen levels are still farther from thermodynamic equilibrium (*7*). This being the case *in situ* energy yield did not


In Aquatic Redox Chemistry; Tratnyek, P., et al.;
ACS Symposium Series; American Chemical Society: Washington, DC, 2011.

Downloaded by UNIV OF GUELPH LIBRARY on October 1, 2011 | http://pubs.acs.org
Publication Date (Web): September 2, 2011 | doi: 10.1021/bk-2011-1071.ch004

reach energy thresholds in empirical studies because $H_2$ concentrations become minute when approaching the threshold (*37*). Enzyme kinetics and limits on diffusive flux probably control $H_2$ concentration and, thus, also *in situ* energy yields of such 'high energy' TEAPs (*37*).

For TEAPs falling into an intermediate range of energy yields, the relationship between energy thresholds and *in situ* energy yields is less uniform. Reduction of chlorinated organics, Cr(VI), As(V), and iron oxides represent examples of these TEAPs. During reductive dechlorination of ethenes, *in situ* energy yields encountered under field or laboratory conditions remained higher than is expected based on the energy thresholds concept (*49*). A similar conclusion has been reached with respect to As(V)-reduction with $H_2$ as electron donor (*29*). With respect to bacterial iron oxide reduction, no coherent picture has emerged so far, potentially caused by the phase transfer reaction and wide range of metastable phases and surface properties of the electron acceptor (*50*). In some cases, microbial reduction of goethite ceased at an energy threshold of around -23 kJ $mol^{-1}$ (*51*), whereas in others experiments no such thresholds could be identified (*52*). An inherent difficulty in studies on iron oxide reduction is the variable nature of the mineral phase, which is altered by sorption, surface precipitation, and catalytic action of ferrous iron (*53*, *54*).

For processes at the low end of energy yields, empirical energy thresholds tended to be fairly consistent and small, and ranged from -20 to -28 kJ $mol^{-1}$, -9 to -50 kJ $mol^{-1}$, and -16 to -49 kJ $mol^{-1}$ for hydrogenotrophic acetogenesis, methanogenesis, and sulfate reduction, respectively (when the reaction was written with the lowest possible integer coefficients) (*6*). The occurrence and kinetics of these processes is, thus, likely controlled by their *in situ* energy yields. The occurrence of these processes at very small $\Delta G_r$ has also been interpreted as an adaptation to survival under "substrate starvation" in depositional environments, where microbial communities are exposed to residual and increasingly recalcitrant organic matter (*41*).

## Energy Thresholds and Transport – Methanogenesis as an Example

A consequence of energy thresholds is the potential for metabolic slowdown by accumulation of metabolic products. Such phenomena are well known from anaerobic bioreactors (*55*). Several closed incubation-type studies have also demonstrated that processes involved in anaerobic respiration slow down or cease when energy thresholds are approached (*41*, *46*, *56*). Extrapolating such experimental observations to peats, Beer et al. (*57*) proposed that small changes in $\Delta G_r$ of methanogenesis by accumulation of DIC and/or $CH_4$ may slow methanogenic decomposition in diffusion dominated methanogenic deposits. In this concept, the production of $CH_4$ reflects a system's limit to accommodate simultaneous constraints of transport, energy, and microbial kinetics.

To test this hypothesis, a simple column experiment was designed with water saturated and anaerobic peat-quartz sand mixtures containing 5%, 15%, and 50% of moderately decomposed peat. Differences in peat quality with depth were eliminated by homogenization and pore water profiles were allowed to approach steady-state in absence of vertical water flow. Under such conditions,


In Aquatic Redox Chemistry; Tratnyek, P., et al.;
ACS Symposium Series; American Chemical Society: Washington, DC, 2011.

Downloaded by UNIV OF GUELPH LIBRARY on October 1, 2011 | http://pubs.acs.org
Publication Date (Web): September 2, 2011 | doi: 10.1021/bk-2011-1071.ch004

$CH_4$ production should diminish to similar and very small values deeper into the deposit regardless of C content, but increase proportionately with C content in the anaerobic layers near the column surface, where the energy constraints are alleviated by continuous removal of DIC and $CH_4$. Furthermore, the decrease in methanogenesis should be related to processes approaching their respective biological energy quantum.

## Methods

### Column Setup and Sampling

Commercially available ombrotrophic bog peat was homogeneously mixed with quartz sand and deionized water, and filled in PVC columns (140 cm x 20 cm) equipped with porewater peepers (*38*) for 120 cm of column length. These could be non-destructively retrieved from perforated and meshed frames embedded in the column filling. Columns were kept dark at 18°C with the water table slightly above the surface. Peepers were retrieved and replaced after 370 and 550 days. DIC, $CH_4$ and $H_2$ concentrations were quantified using headspead techniques, gas chromatography and a Trace Analytical TA 3000 hydrogen analyzer, and converted into dissolved concentration. Inorganic anions (ion chromatography), pH (potentiometry), and $H_2S$ (amperometry) were analyzed as previously described (*38*), and acetate in selected samples was analyzed by HPLC with UV detection at 208 nm.

### Modeling

To model production and transport of $CH_4$ a simple box model was implemented using STELLA© simulation software. The model encompassed 10 fully mixed vertical layers to simulate concentration profiles. Solute transport between layers was simulated using Fick's law with the diffusion coefficient of $CH_4$ taken from (*58*), adjusted to a temperature of 18°C and corrected for the effect of porosity (n) using a factor of $n^2$. The assumption that the system was diffusion dominated was checked by repeated static chamber measurements of $CH_4$ flux (*38*) at the end of the experiments. Ebullition (i.e. bubbling) of $CH_4$,detectable by rapid concentration increase in the chambers, was not observed. Concentrations of $CH_4$ at the upper and lower boundary of column were fixed at measured levels in the model. Porosity was determined from bulk density measurements in separate columns of analogous peat-sand mixtures, as well as estimates of specific density of peat (1.5 g $cm^{-3}$) and quartz components (2.65 g $cm^{-3}$). The production rate of methane in each depth layer was modelled using a modified Michalis-Menten kinetics (equation 1) with a maximum rate $v_{max}$ (µmol $L^{-1}$ $d^{-1}$) and half saturation constant $k_s$ (µmol $L^{-1}$). The model further accounts for the free energy of the process by including the reaction quotient Q and an analogue for the equilibrium constant adjusted to a minimum energy requirement $\Delta G_c$ (kJ $mol^{-1}$ ($CH_4$)). Originally this approach was presented by Hoh and Cord-Ruwisch (*55*) using the equilibrium constant instead. It represents a special case of the more general approach developed by Jin and Bethke (*7*). In the model, the production


In Aquatic Redox Chemistry; Tratnyek, P., et al.;
ACS Symposium Series; American Chemical Society: Washington, DC, 2011.

Downloaded by UNIV OF GUELPH LIBRARY on October 1, 2011 | http://pubs.acs.org
Publication Date (Web): September 2, 2011 | doi: 10.1021/bk-2011-1071.ch004

of methane equals zero when the $Q = K_{threshold}$, i.e. when the energy conserved in ATP generation equals the release of free energy from the overall chemical process. At this point, the thermodynamic driving force becomes zero.

$$-\frac{d[Ac]}{dt} = \frac{d[CH_4]}{dt} = \frac{v_{max}[Ac] \bullet (1 - \frac{Q}{K_{threshold}})}{k_s + [Ac] \bullet (1 + \frac{Q}{K_{threshold}})} \qquad \text{(equation 1)}$$

Gibbs free energy $\Delta G_r$ (kJ mol$^{-1}$) available for hydrogenotrophic (4 $H_2$(aq) + $CO_2$(aq) → 2 $H_2O$(l) + $CH_4$(aq)) and acetoclastic ($CH_3COO^-$(aq) + $H^+$(aq) → $CO_2$(aq) + $CH_4$(aq)) methanogenesis was calculated in the model for the smallest integer stoichiometry using the Nernst equation, as previously described (*38*):

$$\Delta G_r = \Delta G_r^0 + R \cdot T \cdot \ln Q \text{ with } Q = \frac{\prod_i (products)^{\nu_i}}{\prod_i (substrates)^{\nu_i}} \qquad \text{(equation 2)}$$

with $\Delta G_r^0$ the standard Gibbs free energy of the reaction (kJ mol$^{-1}$) at *in situ* temperature of 18°C, R the gas constant ($8.314 \times 10^{-3}$ kJ mol$^{-1}$ K$^{-1}$), T the absolute temperature (K), and ν the stoichiometric coefficients. The pressure dependency of $\Delta G_r$ and the effect of ionic strength on activities were neglected.

Hydrogenotrophic methanogenesis provided insufficient free energy for methanogenesis, at least at the spatial scale of solute sampling (data not shown). The model was thus restricted to the utilization of acetate and parameterized in agreement with literature ranges of $v_{max}$, $k_s$, and the critical energy converted to a $K_{threshold}$. Parameterization was further attempted with one consistent set of parameters for simulating $CH_4$ concentration profiles in 5 %, 15%, and 50% peat columns at 370 and 550 days, simultaneously. To account for an initial utilization of electron acceptors after flooding (*59*), a time lag of 100 days was assumed before methane production began and reached full production after 200 days. Acetate concentration was fixed at average levels of 10 µmol L$^{-1}$, or about half the detection limit of measurements. The DIC, here equivalent to dissolved $CO_2$, concentration profiles were simulated simultaneously using (1) first order kinetics of DIC production and decomposition constants of 0.0018 to 0.0028 d$^{-1}$ to match the observed accumulation of DIC, and (2) an empirical linearly-increasing inhibition of DIC production at levels of 5000 to 10500 µmol L$^{-1}$, which was needed to match the evolution of DIC profiles in the experiments (data not shown).

The Michaelis-Menten model was also applied without the energy threshold to test if $CH_4$ profiles across the columns and over time could be created without a thermodynamic inhibition of acetoclastic methanogenesis. Finally, sensitivity analyses were carried out regarding $v_{max}$, $k_s$, $\Delta G_c$, and concentrations of acetate.

Downloaded by UNIV OF GUELPH LIBRARY on October 1, 2011 | http://pubs.acs.org
Publication Date (Web): September 2, 2011 | doi: 10.1021/bk-2011-1071.ch004

## Results and Discussion

### Concentration Dynamics

Methane concentration in the peat columns increased with depth and time in all three peat sand mixtures (Figure 2). Concentrations reached 280 to 500 µmol $L^{-1}$ (5% peat), 400 to 500 µmol $L^{-1}$ (15 % peat), and 600 µmol $L^{-1}$ (50% peat) in the columns. In the 50 % peat column concentrations hardly increased between 370 d and 550 d sampling; this column was near steady state by the end of the experiment, whereas concentration moderately increased in the 15%, and strongly increased in the 5% peat column.

Downloaded by UNIV OF GUELPH LIBRARY on October 1, 2011 | http://pubs.acs.org
Publication Date (Web): September 2, 2011 | doi: 10.1021/bk-2011-1071.ch004

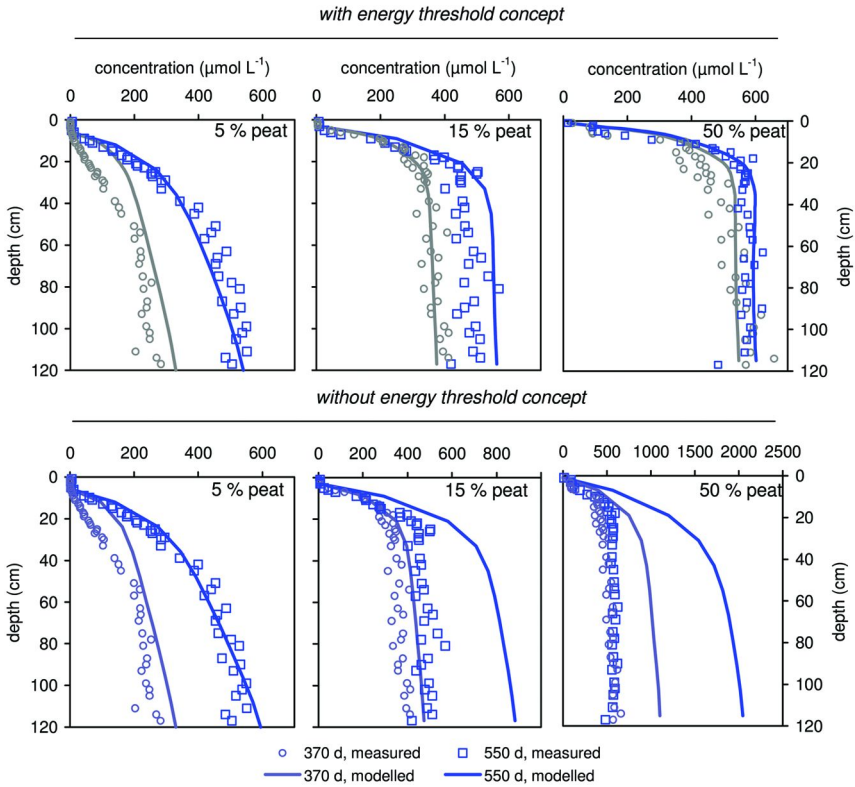



*Figure 2. Measured and modelled $CH_4$ concentrations in experiments with 5% peat, 15% peat, and 50% peat (mass basis) in homogenized peat - quarz sand mixtures after 370 days and 550 days of incubation. Note different concentration scales. In the uppermost series of simulations, an energy threshold at -25 kJ mol-1 ($CH_4$) was implemented, resulting in slow down of concentration increase and the 'flattening' of the profiles observed with depth. In the lower panels, this constraint was removed.*


In Aquatic Redox Chemistry; Tratnyek, P., et al.;
ACS Symposium Series; American Chemical Society: Washington, DC, 2011.

Strikingly, the methane concentration increase with depth levelled off when the concentration profiles approached steady state, indicating an absence of methane production deeper into the peat sand mixtures. DIC concentrations increased in a similar but less steep manner to maximum levels of 5500 µmol $L^{-1}$, 8500 µmol $L^{-1}$, and 9500 µmol $L^{-1}$; $H_2$ concentrations varied from 0.1 to 2.7 nmol $L^{-1}$; and acetate concentration remained below the limit of detection. Values of pH were slightly to moderately acidic and ranged from 4.0 to 5.4, generally increasing with depth.

The methane dynamics in the columns could be adequately reproduced with the model that included an energy threshold of -25 kJ $mol^{-1}$ ($CH_4$) and reasonably consistent $V_{max}$ and $k_s$ values that were in the broad range reported for peats and similar substrates (Figure 2). Values of $k_s$ have been reported to be between 5 and 200 µmol $L^{-1}$ (*60*); a value of 10 µmol $L^{-1}$ was used in all simulations. A best fit could be reached when $V_{max}$ increased from 6.5 µmol $L^{-1}$ $d^{-1}$ (5% peat), 11 µmol $L^{-1}$ $d^{-1}$ (15% peat) to 36.8 µmol $L^{-1}$ $d^{-1}$ (50% peat). Such values are well in line with measured *in situ* $CH_4$ production in similar bog peats during summer (*61*). Between the 15% and 50% treatments the increase in $V_{max}$ was proportionate to the increase in organic matter content. Successful reproduction of the $CH_4$ profiles in the 5% treatment required a somewhat higher $V_{max}$ than proportional to the differences in peat content. Acetate concentrations averaged 10 µmol $L^{-1}$ in all model columns, but some adjustment of concentration levels with depth was required. In the 15 % and 50 % columns, a good fit was reached with a linear increase from 8.6 µmol $L^{-1}$ to 11.4 µmol $L^{-1}$, whereas in the 5% column concentrations increased linearly from 5.5 to 14.5 µmol $L^{-1}$, resulting in faster rising $CH_4$ concentration deeper into the peat of this column (Figure 2). These assumptions are arbitrary but within the boundary stipulated by the acetate analyses.

Importantly, methane dynamics could not be reproduced across time and peat content without an energy threshold ($\Delta G_c$) (Figure 2). In any particular column, a $CH_4$ profile could be adequately fitted by some parameter combination. In the 5% treatment, this exercise succeeded for both profiles at 370 d and 550 d (Figure 2). However, in the 15% and 50% treatments, a good fit of the 550 d profiles resulted in gross underestimates of concentrations after 370 d (data not shown). Using the general parameterization that produced a good fit in the 5% peat column, $CH_4$ concentrations in the other columns were strongly overestimated in absence of an energy threshold (Figure 2). While there is considerably degree of freedom in the model parameterization, these results suggest that a threshold to $CH_4$ production was present. This threshold was not yet reached in the 5%, but clearly reached in the 15% and particularly the 50% peat column. The nature of this threshold cannot be unequivocally ascertained, but the fact that it occurred when Gibbs free energies of acetoclastic methanogenesis reached -25 kJ $mol^{-1}$ (which is close to theoretical energy thresholds (*5*)) suggest that methane production and increase in methane concentrations was inhibited thermodynamically and ultimately by the slowness of diffusive transport removing $CH_4$ and DIC.

Downloaded by UNIV OF GUELPH LIBRARY on October 1, 2011 | http://pubs.acs.org
Publication Date (Web): September 2, 2011 | doi: 10.1021/bk-2011-1071.ch004

Downloaded by UNIV OF GUELPH LIBRARY on October 1, 2011 | http://pubs.acs.org
Publication Date (Web): September 2, 2011 | doi: 10.1021/bk-2011-1071.ch004

**Production Rates and Parameter Sensitivity**

Some further insight into the methane production dynamics leading to this phenomenon can be gained by analyzing profiles of $CH_4$ production and Gibbs free energy in the model (Figure 3), as well as the sensitivity to processes to the parameters (Figure 4). In the 5% model, $CH_4$ production only slightly decreased over time and $\Delta G_r$ remained < -28 kJ $mol^{-1}$ (Figure 3). In the 50% peat model, methane production remained strong in the uppermost layer under the same $\Delta G_r$, whereas at larger depth production declined to zero. The 15% peat model was characterized by a more moderate inhibition of methanogenesis with time and depth. The decline of methanogenesis to zero in the 50% peat model was essentially caused by lower DIC concentration in the upper part of the column, which allowed for higher $CH_4$ concentrations at the energy threshold (see also equation (2)).

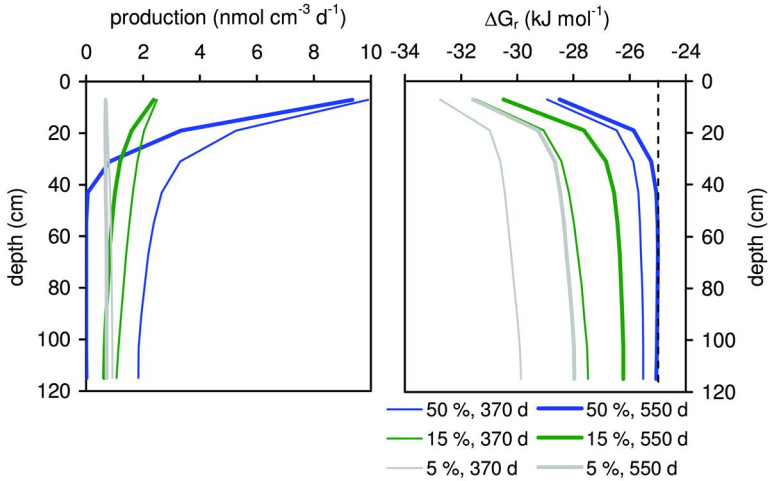



*Figure 3. Modelled depth profiles of $CH_4$ production and respective $\Delta G_r$ of the processes at 370 and 550 days of incubation in experiments with 5% peat, 15% peat, and 50 % peat in homogenized peat - quarz sand mixtures.*

As a result, $CH_4$ concentration slightly peaked at about 30 cm depth (Figure 2), where the gas diffused mostly upwards but also slightly downward, thus raising $CH_4$ concentration in deeper layers to levels that did not allow for any further production. This created the remarkably straight $CH_4$ concentration depth profiles in the model that were also observed in the empirical data (Figure 2).

The sensitivity analysis illustrates that concentration profiles were highly dependent on both the energy threshold and substrate concentration, and to a lesser degree on the kinetic $V_{max}$ and $k_s$ values. This assumes a reasonable range of these parameters in anoxic environments and confirms earlier studies (*55*). The finding is exemplified in the 50% peat column after 550 d (Figure 4). In each of the analyses, all parameters except one were kept constant.

Downloaded by UNIV OF GUELPH LIBRARY on October 1, 2011 | http://pubs.acs.org
Publication Date (Web): September 2, 2011 | doi: 10.1021/bk-2011-1071.ch004

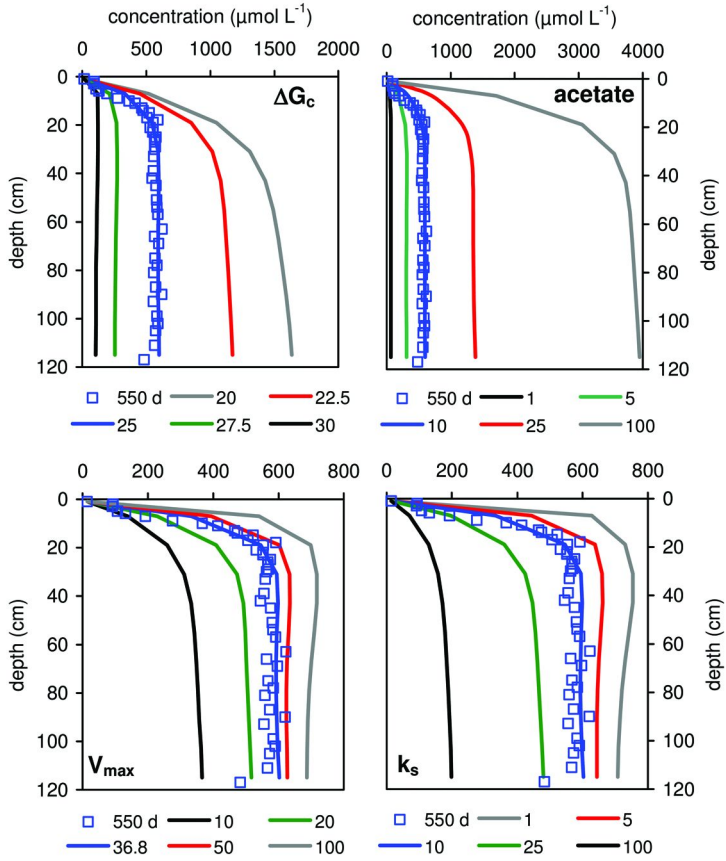



*Figure 4. Sensitivity of modeled $CH_4$ concentrations in 50 % peat columns to changes in threshold energy $\Delta G_c$, acetate concentration, maximum production rate $V_{max}$, and half saturation constant $k_s$, while keeping all other parameters constant in each simulation. When not varied in a simulation, $\Delta G_c$= 25 kJ mol$^{-1}$, $V_{max}$ =36.8 µmol L$^{-1}$ d$^{-1}$, acetate = 10 µmol L$^{-1}$, and $k_s$ = 0.0028 d$^{-1}$.*

Moderate changes in the physiologically based energy threshold of ± 5 kJ mol$^{-1}$, which are smaller than widely reported and may reflect adaptations to the general availability of substrates (*6*), can thus lead to very different steady state $CH_4$ levels in methanogenic peat deposits, which may contribute to large variations that have reported from field sites (*57*, *62*). A similarly strong influence of acetate concentration on the $CH_4$ concentrations was observed at an energy threshold of -25 kJ mol$^{-1}$. The parameters $V_{max}$ and $k_s$ primarily influenced the temporal dynamics in the model, i.e. the time required for $CH_4$ profiles to reach steady state near the energy threshold (Figure 4). Higher $V_{max}$ and $k_s$ also reinforce the already described phenomenon of increases of $CH_4$ concentrations beyond levels stipulated by $\Delta G_c$ in lower depths of this semi-closed soil system. This is caused by more vigorous $CH_4$ production in the upper layers, where DIC concentrations

are lower than in larger depths, thus allowing for higher $CH_4$ concentrations at the energy threshold.

The effect of acetate concentration on $CH_4$ concentration levels stresses the importance of the dynamic equilibrium between acetate production and methanogenic consumption near energy thresholds. This point is further illustrated in Figure 5, which shows $\Delta G_r$ available for the fermenatation of propionate to acetate and its subsequent consumption by acetoclastic methanogenesis over a range of DIC, i.e. dissolved $CO_2$, and $CH_4$ concentrations. Whereas at low DIC and $CH_4$ concentrations both processes can occur over a wide range of acetate concentrations, in the example between 0.1 and 10 µmol $L^{-1}$, this range decreases with accumulation of DIC and $CH_4$ to a narrow band near 10 µmol $L^{-1}$. Deviation from this band would inhibit either process, and the effect of higher acetate concentration could only be compensated for by elevating concentrations of propionate. The 'energy signal' of DIC and $CH_4$ accumulation may be distributed through the preceding fermentation network, which could, for example, help to explain high levels of acetate and propionate in groundwater systems (*57*, *63*). Thus, temporary or local increases of acetate concentrations that have been widely reported for example in wetland (*64*, *65*) and aquifer systems (*63*, *66*) have the potential to ease thermodynamic constraints on acetoclastic methanogenesis, but, on the other hand, may inhibit preceding fermentation processes, as suggested in organic rich peat aquifers (*38*, *57*).

Downloaded by UNIV OF GUELPH LIBRARY on October 1, 2011 | http://pubs.acs.org
Publication Date (Web): September 2, 2011 | doi: 10.1021/bk-2011-1071.ch004

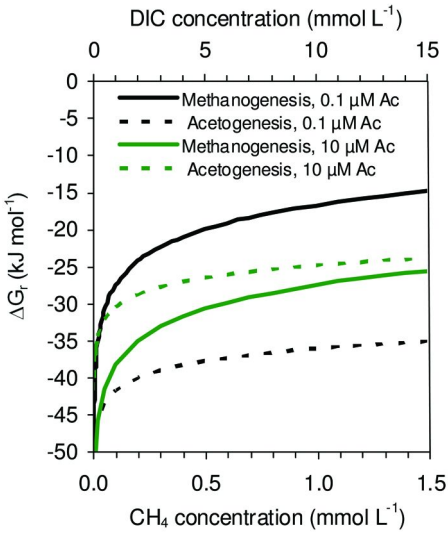



*Figure 5. Gibbs free energy $\Delta G_r$ available from acetoclastic methanogenesis and syntrophic propionate fermentation to acetate ($CH_3CH_2COOH$ (aq) + $2H_2O$ (l) ⇌ $CH_3COOH$ (aq) + $CO_2$ (aq) + 3 $H_2$ (aq)) with increasing DIC and $CH_4$ concentration. Assuming propionate concentrations of 1 µmol $L^{-1}$ and either 0.1 or 10 µmol $L^{-1}$ of acetate. DIC is assumed to be dissolved $CO_2$.*


In Aquatic Redox Chemistry; Tratnyek, P., et al.;
ACS Symposium Series; American Chemical Society: Washington, DC, 2011.

## Conclusions

This review and case study demonstrate the usefulness of considering the energy threshold concept when interpreting the occurrence, rate and spatio-temporal distribution of $H_2$ and organic acid dependent TEAPs and methanogenesis in anoxic systems. $H_2$-dependent methanogenesis and sulfate reduction typically operate near free energy thresholds ($\Delta G_c$) in soils and sediments, and can thus be inhibited by changes in geochemical conditions that are induced by constraints on transport of solutes and by provision of TEAPs that are energetically more potent. These TEAPS operate far from theoretical energy thresholds, despite higher physiological energy threshold levels, and can lower $H_2$ concentrations to levels excluding less potent TEAPs. Energy thresholds are dependent on microbial physiology and occur when the energy conserved by ATP generation comes close to the thermodynamic driving force. The case study illustrates that accumulation of methane in diffusion dominated and DIC rich systems may cause inhibition of acetoclastic methanogenesis near energy thresholds, and the high sensitivity of such a mechanism to small changes in acetate concentration and the energy threshold $\Delta G_c$. The production and flux of $CH_4$, as the most reduced metabolic product of anaerobic organic matter decomposition, appeared to reflect the system's ability to simultaneously adjust to transport, energy, and microbial kinetic constraints on the redox process. Low energy, in particular methanogenic, systems may thus operate in a mode in which processes and constraints converge towards a characteristic steady state that reflects a specific capacity to process organic material and that is likely highly dependent on rates of solute transport.

Downloaded by UNIV OF GUELPH LIBRARY on October 1, 2011 | http://pubs.acs.org
Publication Date (Web): September 2, 2011 | doi: 10.1021/bk-2011-1071.ch004

## Acknowledgments

I gratefully acknowledge the technical support by M. Heider, H. Zier, S. Hammer, L.Likke, and D. Burghardt, and contributions made by M. Siems and J. Beer to data analysis.

## References

1. Lovley, D. R.; Coates, J. D. Novel forms of anaerobic respiration of environmental relevance. *Curr. Opin. Microbiol.* **2000**, *3* (3), 252–256.
2. Appelo, C. A. J.; Postma, D. *Geochemistry, groundwater and pollution*, 2nd ed.; A. A. Balkema Publishers: Leiden, The Netherlands, 2005; p 649.
3. Froehlich, P. N.; Klinkhammer, G. P.; Bender, M. L.; Luedke, N. A.; Heath, G. R.; Gullen, D.; Dauphin, P.; Hammond, D.; Hartman, B. Early oxidation of organic matter in pelagic sediments of the eastern equatorial Atlantic: suboxic diagenesis. *Geochim. Cosmochim. Acta* **1979**, *43*, 1075–1090.
4. Thauer, R. K.; Jungermann, K.; Decker, K. Energy-Conservation in Chemotropic Anaerobic Bacteria. *Bacteriol. Rev.* **1977**, *41* (1), 100–180.
5. Schink, B. Energetics of syntrophic cooperation in methanogenic degradation. *Microbiol. Mol. Biol. Rev.* **1997**, *61* (2), 262–280.

6. Hoehler, T. M. Biological energy requirements as quantitative boundary conditions for life in the subsurface. *Geobiology* **2004**, *2*, 205–215.
7. Jin, Q. S.; Bethke, C. M. Predicting the rate of microbial respiration in geochemical environments. *Geochim. Cosmochim. Acta* **2005**, *69* (5), 1133–1143.
8. Jakobsen, R. Redox microniches in groundwater: A model study on the geometric and kinetic conditions required for concomitant Fe oxide reduction, sulfate reduction, and methanogenesis. *Water Resour. Res.* **2007**, *43*, W12S12; doi:10.1029/2006WR005663.
9. Fenchel, T.; King, G. M.; Blackburn, T. H. *Bacterial Biogeochemistry*; Academic Press: London, 1998.
10. Decad, G. M.; Nikaido, H. Outer membrane of gram-negative bacteria. XII Molecular-sieving function of cell wall. *J. Bacteriol.* **1976**, *128*, 325–336.
11. Conrad, R. Contribution of hydrogen to methane production and control of hydrogen concentrations in methanogenic soils and sediments. *FEMS Microbiol. Ecol.* **1999**, *28* (3), 193–202.
12. Vignais, P. M.; Colbeau, A. Molecular biology of microbial hydrogenases. *Curr. Issues Mol. Biol.* **2004**, *6*, 159–188.
13. Hering, J.; Hug, S. J.; Farnsworth, C.; O'Day, P. A. Role of coupled redox transformations in the mobilization and sequestration of arsenic. In *Aquatic Redox Chemistry*, Tratnyek, P., Grundl, T. J., Haderlein, S. B., Eds.; American Chemical Society: Washington, DC, 2011; Vol. 1071, Chapter 21, pp 463−476.
14. O'Loughlin, E. J.; Boyanov, M. I.; Antonopoulos, D. A.; Kemner, K. M. Redox processes affecting the speciation of technetium, uranium, neptunium, and plutonium in aquatic and terrestrial environments. In *Aquatic Redox Chemistry*, Tratnyek, P., Grundl, T. J., Haderlein, S. B., Eds.; American Chemical Society: Washington, DC, 2011; Vol. 1071, Chapter 22, pp 477−517.
15. Conrad, R.; Goodwin, S.; Zeikus, J. G. Hydrogen metabolism in a mildly acidic lake sediment (Knaack Lake). *FEMS Microbiol. Ecol.* **1987**, *45* (4), 243–249.
16. Kurtz, W.; Peiffer, S., The role of transport in aquatic redox chemistry. In *Aquatic Redox Chemistry*, Tratnyek, P., Grundl, T. J., Haderlein, S. B., Eds.; American Chemical Society: Washington, DC, 2011; Vol. 1071, Chapter 25, pp 559−580.
17. Lovley, D. R.; Goodwin, S. Hydrogen concentrations as an indicator of the predominant terminal electron accepting reactions in aquatic sediments. *Geochim. Cosmochim. Acta* **1988**, *52*, 2993–3003.
18. Lovley, D. R.; Chapelle, F. H. Deep subsurface microbial processes. *Rev. Geophys.* **1995**, *33* (3), 365–381.
19. Chapelle, F. H.; Lovley, D. R. Competitive exclusion of sulfate reduction by Fe(III)-reducing bacteria: a mechanism for producing discrete zones of high-iron ground water. *Ground Water* **1992**, *30* (1), 29–36.
20. Heimann, A.; Jakobsen, R.; Blodau, C. Energetic constraints on $H_2$-dependent terminal electron accepting processes in anoxic environments

Downloaded by UNIV OF GUELPH LIBRARY on October 1, 2011 | http://pubs.acs.org
Publication Date (Web): September 2, 2011 | doi: 10.1021/bk-2011-1071.ch004

- a review of observations and model approaches. *Environ. Sci. Technol.* **2010**, *44* (1), 24–33.
21. Vroblesky, D. A.; Chapelle, F. H. Temporal and spatial changes of terminal electron-accepting processes in a petroleum hydrocarbon-contaminated aquifer and the significance for contaminant biodegradation. *Water Resour. Res.* **1994**, *30* (5), 1561–1570.
22. Chapelle, F. H.; McMahon, P. B.; Dubrovsky, N. M.; Fujii, R. F.; Oaksford, E. T.; Vroblesky, D. A. Deducing the distribution of terminal electron-accepting processes in hydrologically diverse groundwater systems. *Water Resour. Res.* **1995**, *31* (2), 359–371.
23. Christensen, T. H.; Bjerg, P. L.; Banwart, S. A.; Jakobsen, R.; Heron, G.; Albrechtsen, H. J. Characterization of redox conditions in groundwater contaminant plumes. *J. Contam. Hydrol.* **2000**, *45* (3−4), 165–241.
24. Gonsoulin, M. E.; Wilson, B. H.; Wilson, J. T. Biodegradation of PCE and TCE in landfill leachate predicted from concentrations of molecular hydrogen: a case study. *Biodegradation* **2004**, *15* (6), 475–485.
25. Lovley, D. R.; Phillips, E. J. P. Competitive mechanisms for inhibition of sulfate reduction and methane production in the zone of ferric iron reduction in sediments. *Appl. Environ. Microbiol.* **1987**, *53* (11), 2636–2641.
26. Stumm, W.; Morgan, J. J. *Aquatic chemistry - chemical equilibria and rates in natural waters*; Wiley-Interscience: New York, 1996.
27. Krauskopf, K. B.; Bird, D. K. *Introduction to Geochemistry*, 3rd ed.; McGraw-Hill: 1994; p 640.
28. Thauer, R. K.; Jungermann, K.; Decker, K. Energy conservation in chemotrophic anaerobic bacteria. *Bacteriol. Rev.* **1977**, *41* (1), 100–180.
29. Heimann, A.; Blodau, C.; Postma, D.; Larsen, F.; Viet, P. H.; Nhan, P. Q.; Jessen, S.; Duc, M. T.; Hue, N. T. M.; Jakobsen, R. Hydrogen thresholds and steady state concentrations associated with microbial arsenate respiration. *Environ. Sci. Technol.* **2007**, *41*, 2311–2317.
30. Jakobsen, R.; Albrechtsen, H. J.; Rasmussen, M.; Bay, H.; Bjerg, P. L.; Christensen, T. H. $H_2$ concentrations in a landfill leachate plume (Grindsted, Denmark): In situ energetics of terminal electron acceptor processes. *Environ. Sci. Technol.* **1998**, *32* (14), 2142–2148.
31. McGuire, J. T.; Smith, E. W.; Long, D. T.; Hyndman, D. W.; Haack, S. K.; Klug, M. J.; Velbel, M. A. Temporal variations in parameters reflecting terminal-electron-accepting processes in an aquifer contaminated with waste fuel and chlorinated solvents. *Chem. Geol.* **2000**, *169* (3−4), 471–485.
32. Cozzarelli, I. M.; Suflita, J. M.; Ulrich, G. A.; Harris, S. H.; Scholl, M. A.; Schlottmann, J. L.; Christenson, S. Geochemical and microbiological methods for evaluating anaerobic processes in an aquifer contaminated by landfill leachate. *Environ. Sci. Technol.* **2000**, *34* (18), 4025–4033.
33. Hansen, L. K.; Jakobsen, R.; Postma, D. Methanogenesis in a shallow sandy aquifer, Romo, Denmark. *Geochim. Cosmochim. Acta* **2001**, *65* (17), 2925–2935.
34. Watson, I. A.; Oswald, S. E.; Mayer, K. U.; Wu, Y. X.; Banwart, S. A. Modeling kinetic processes controlling hydrogen and acetate concentrations

Downloaded by UNIV OF GUELPH LIBRARY on October 1, 2011 | http://pubs.acs.org
Publication Date (Web): September 2, 2011 | doi: 10.1021/bk-2011-1071.ch004

Downloaded by UNIV OF GUELPH LIBRARY on October 1, 2011 | http://pubs.acs.org
Publication Date (Web): September 2, 2011 | doi: 10.1021/bk-2011-1071.ch004

in an aquifer-derived microcosm. *Environ. Sci. Technol.* **2003**, *37* (17), 3910–3919.
35. Broholm, M. M.; Crouzet, C.; Arvin, E.; Mouvet, C. Concurrent nitrate and Fe(III) reduction during anaerobic biodegradation of phenols in a sandstone aquifer. *J. Contam. Hydrol.* **2000**, *44* (3-4), 275–300.
36. Jakobsen, R.; Postma, D. Redox zoning, rates of sulfate reduction and interactions with Fe-reduction and methanogenesis in a shallow sandy aquifer, Romo, Denmark. *Geochim. Cosmochim. Acta* **1999**, *63* (1), 137–151.
37. Hoehler, T. M.; Alperin, M. J.; Albert, D. B.; Martens, C. S. Thermodynamic control on hydrogen concentrations in anoxic sediments. *Geochim. Cosmochim. Acta* **1998**, *62* (10), 1745–1756.
38. Beer, J.; Blodau, C. Transport and thermodynamics constrain belowground carbon turnover in a northern peatland. *Geochim. Cosmochim. Acta* **2007**, *71*, 2989–3002.
39. Rothfuss, F.; Conrad, R. Thermodynamics of methanogenic intermediary metabolism in littoral sediment of Lake Constance. *FEMS Microbiol. Ecol.* **1993**, *12* (4), 265–276.
40. Chin, K.-J.; Conrad, R. Intermediary metabolism in methanogenic paddy soil and the influence of temperature. *FEMS Microbiol. Ecol.* **1995**, *18* (2), 85–102.
41. Hoehler, T. M.; Alperin, M. J.; Albert, D. B.; Martens, C. S. Apparent minimum free energy requirements for methanogenic Archaea and sulfate-reducing bacteria in an anoxic marine sediment. *FEMS Microbiol. Ecol.* **2001**, *38* (1), 33–41.
42. Nicholls, D. G.; Ferguson, S. J. *Bioenergetics 3*, 3rd ed.; Academic Press, Elsevier Science: 2002.
43. Valentine, D. L. Adaptations to energy stress dictate the ecology and evolution of the Archaea. *Nat. Rev. Microbiol.* **2007**, *5* (4), 316–323.
44. Mulkidjanian, A. Y.; Dibrov, P.; Galperin, M. Y. The past and present of sodium energetics: May the sodium-motive force be with you. *Biochim. Biophys. Acta, Bioenerg.* **2008**, *1777*, 985–992.
45. Becher, B.; Muller, V. Delta-mu(Na+) drives the synthesis of ATP via an delta-mu(Na+)-translocating F1F0-ATP synthase in membrane-vesicles of the Archaeon *Methanosarcina mazei* Go1. *J. Bacteriol.* **1994**, *176* (9), 2543–2550.
46. Jackson, B. E.; McInerney, M. J. Anaerobic microbial metabolism can proceed close to thermodynamic limits. *Nature* **2002**, *415* (6870), 454–456.
47. Drake, H. L.; Küsel, K.; Mathiess, C. Acetogenic Prokaryotes. *Prokaryotes* **2006**, *2*, 355–420.
48. Kleerebezem, R.; Stams, A. J. M. Kinetics of syntrophic cultures: A theoretical treatise on butyrate fermentation. *Biotechnol. Bioeng.* **2000**, *67* (5), 529–543.
49. Heimann, A.; Jakobsen, R. Experimental evidence for a lack of thermodynamic control on hydrogen concentrations during anaerobic degradation of chlorinated ethenes. *Environ. Sci. Technol.* **2006**, *40* (11), 3501–3507.

50. Kocar, B.; Fendorf, S. Thermodynamic constraints on reductive reactions influencing the biogeochemistry of arsenic in soils and sediments. *Environ. Sci. Technol.* **2009**, *43*, 4871–4877.
51. Liu, C. X.; Kota, S.; Zachara, J. M.; Fredrickson, J. K.; Brinkman, C. K. Kinetic analysis of the bacterial reduction of goethite. *Environ. Sci. Technol.* **2001**, *35* (12), 2482–2490.
52. Roden, E. E. Diversion of electron flow from methanogenesis to crystalline Fe(III) oxide reduction in carbon-limited cultures of wetland sediment microorganisms. *Appl. Environ. Microbiol.* **2003**, *69* (9), 5702–5706.
53. Roden, E. E.; Urrutia, M. M. Influence of biogenic Fe(II) on bacterial crystalline Fe(III)oxide reduction. *Geomicrobiol. J.* **2002**, *19*, 209–251.
54. Pedersen, H. D.; Postma, D.; Jakobsen, R.; Larsen, O. Fast transformation of iron oxyhydroxides by the catalytic action of aqueous Fe(II). *Geochim. Cosmochim. Acta* **2005**, *69* (16), 3967–3977.
55. Hoh, C. Y.; Cord-Ruwisch, R. A practical kinetic model that considers endproduct inhibition in anaerobic digestion processes by including the equilibrium constant. *Biotechnol. Bioeng.* **1996**, *51* (5), 597–604.
56. Krylova, N. I.; Conrad, R. Thermodynamics of propionate degradation in methanogenic paddy soil. *FEMS Microbiol. Ecol.* **1998**, *26* (4), 281–288.
57. Beer, J.; Lee, K.; Whiticar, M.; Blodau, C. Geochemical controls on anaerobic organic matter decomposition in a northern peatland. *Limnol. Oceanogr.* **2008**, *53* (4), 1393–1407.
58. Lerman, A. *Geochemical Processes - Water and Sediment Environments*; Krieger: Malabar, FL, 1988.
59. Blodau, C.; Moore, T. R. Experimental response of peatland carbon dynamics to a water fluctuation. *Aquat. Sci.* **2003**, *65*, 47–62.
60. Segers, R. Methane production and methane consumption: a review of processes underlying wetland methane fluxes. *Biogeochemistry* **1998**, *41* (1), 23–51.
61. Blodau, C.; Roulet, N. T.; Heitmann, T.; Stewart, H.; Beer, J.; Lafleur, P.; Moore, T. R. Belowground carbon turnover in a temperate ombrotrophic bog. *Global Biogeochem. Cycles* **2007**, *21* (1), GB1021.
62. Chasar, L. S.; Chanton, J. P.; Glaser, P. H.; Siegel, D. I.; Rivers, J. S. Radiocarbon and stable carbon isotopic evidence for transport and transformation of dissolved organic carbon, dissolved inorganic carbon, and $CH_4$ in a northern Minnesota peatland. *Global Biogeochem. Cycles* **2000**, *14* (4), 1095–1108.
63. McMahon, P. B.; Chapelle, F. H. Microbial production of organic acids in aquitard sediments and its role in aquifer geochemistry. *Nature* **1991**, *349*, 233–235.
64. Duddleston, K. N.; Kinney, M. A.; Kiene, R. P.; Hines, M. E. Anaerobic microbial biogeochemistry in a northern bog: Acetate as a dominant metabolic end product. *Global Biogeochem. Cycles* **2002**, *16* (4), 1–9.
65. Shannon, R. D.; White, J. R. The effects of spatial and temporal variations in acetate and sulfate on methane cycling in two Michigan peatlands. *Limnol. Oceanogr.* **1996**, *41* (3), 435–443.

Downloaded by UNIV OF GUELPH LIBRARY on October 1, 2011 | http://pubs.acs.org
Publication Date (Web): September 2, 2011 | doi: 10.1021/bk-2011-1071.ch004

66. Chapelle, F. H.; Bradley, P. M. Microbial acetogenesis as a source of organic acids in ancient Atlantic Coastal Plain sediments. *Geology* **1996**, *24*, 925–928.

Downloaded by UNIV OF GUELPH LIBRARY on October 1, 2011 | http://pubs.acs.org
Publication Date (Web): September 2, 2011 | doi: 10.1021/bk-2011-1071.ch004